Peer-reviewed version available at *Materials* **2019**, *12*, 3051; doi:10.3390/ma12183051

Formation of Hierarchical Porous Films with Breath-Figures Self-Assembly Performed on Oil-Lubricated Substrates

Edward Bormashenko, Yelena Bormashenko, Mark Frenkel
[1] Department of Chemical Engineering, Biotechnology and Materials, Engineering Sciences Faculty, Ariel University, Ariel, Israel 407000

***** Correspondence: Dr. Edward Bormashenko: edward@ariel.ac.il ; Tel.: +972 074 729 68 63

Abstract

Hierarchical honeycomb patterns were manufactured with the breath-figures self-assembly by drop-casting on the silicone-oil lubricated glass substrates. Silicone oil promoted spreading of the polymer solutions. The process was carried out with the industrial grade polystyrene and polystyrene with the molecular weight $M_w = 35.000$. Both of polymers gave rise to the patterns, built from micro- and nano-scaled pores. Ordering of the pores was quantified with the Voronoi tessellations and calculating the Voronoi entropy. Measurement of the apparent contact angles evidenced the Cassie - Baxter wetting regime of the porous films.

Keywords: honeycomb polymer films; breath figures self-assembly; oil-lubricated substrates; Voronoi entropy; Cassie wetting regime

1. Introduction

An interest to micro-patterned surfaces has been increased in last decades due to their significant role in a variety of technologies, including biotechnology [1] , tribology [2], optical [3] and microfluidics [4] applications. Micro-patterned surfaces enable the control of lining cells' position, shape and function [1], constituting of dry and wet friction [2], design of the surfaces with prescribed optical properties [3] and smart manipulation of micro-volumes of liquids [4] . Manufacturing of micro-patterned surfaces is a key factor for industry implementation of biomimetic-inspired effects such as the lotus- and shark skin-effects, allowing preparing superhydrophobic interfaces [5,6] and surfaces

Peer-reviewed version available at Materials 2019, 12, 3051; doi:10.3390/ma12183051

demonstrating low hydrodynamic drag [7]. A variety of advanced techniques have been implemented for manufacturing micro-patterned surfaces, including micro-printing [1], replica molding [3,8] , photolithography, molecular assembly patterning, stencil-assisted patterning, ink-jet technology, laser-guided writing of patterns and exploiting surface instabilities [9-11].

One of the simplest and most effective methods enabling manufacturing micro-porous surfaces is the so-called breath-figures self-assembly method [12-17]. Breath-figures process is a commonly observed phenomenon in daily life. One example is the fog that appears on a window when we breathe on it [18]. This is also the origin of the name "breath figure". In the modern era systematic study of the process of breath-figures water condensation was carried out by Aitken [19], Rayleigh [20] and Baker [21]. The interest to the breath-figures process was revived when it was demonstrated that water condensation occurring under evaporation of rapidly evaporated polymer solutions results in formation of well-ordered, micro-porous, honeycomb patterns [23-26]. These patterns demonstrated a potential for photonics [27-29], membranes [30] and biotechnology [31]. We demonstrate the possibility to manufacture hierarchical porous structures with the breath-figures self-assembly realized with oil-lubricated surfaces.

2. Materials and Methods.

2.1. Materials

Two kinds of polystyrene (PS) were used for the breath figures self-assembly. The first of them PS with molecular mass $M_w = 35.000$ supplied by Sigma-Aldrich. The second was industrial PS, supplied by BASF SE. Silicone oil (Poly(dimethylsiloxane, PDMS)) supplied by Sigma-Aldrich with average $M_n = 580$ and density $\rho = 0.93 \frac{g}{cm^3}$ was used as a lubricator. Glass slides 18x18 mm with the thickness of 150 µm were used as solid substrates. Mixture of Dichloromethane (CH_2Cl_2) and Chloroform ($CHCl_3$) was used as a solvent. Chemical grade solvents were supplied by Bio-Lab ltd. A 4 wt.% PS solution was prepared by dissolving the polymer in a mixture of chloroform (7.6 wt.%) and dichloromethane (87.4 wt.%).

2.2. Methods

2.2.1. Preparing of silicone oil lubricated glass substrates

Glass slides were pre-treated (de-greased and hydrophilized) with the plasma unit EQ-PDC-326 manufactured by MTI Co, USA equipped with a dry vacuum pump and pressure gauge EDWARDS 655AB. Glass slides were exposed to an inductive air plasma discharge under the following parameters: the plasma frequency was 13.56 MHz; the pressure was 1 Torr; the supplied power of plasma discharge was 18 W. The time span of irradiation was 120s. Silicone oil (PDMS) was uniformly spread on the hydrophilized slide glass and formed the layer with the thickness of 3.8±0.1 μm, as established by weighting.

2.2.2. Breath-figures self-assembly under drop-casting of polymer solutions onto silicone oil-lubricated substrates

The polymer solution prepared as described in Section 2.1 was cast by dropping on the silicone oil lubricated glass slide, as shown in **Figure 1**. The volume of the droplet was 30 μl. The process of drop-casting was carried under the temperature of 25ºC, and relative humidity RH=40%.

2.2.3. Characterization of the topography of the patterns

The topography of samples was studied with the SWIFT M4000D optical microscope and Ultra-High Resolution MAIA3 FE-SEM device. The ordering of pores was quantified with Voronoi tessellations performed with the moduli of the MATLAB program developed at the Department of Physics and Astronomy at the University of California (https://www.physics.uci.edu/~foams/do_all.html).

2.2.4. Characterization of the wetting mode of the breath figures honeycomb patterns

Apparent contact angles were measured with the goniometer Rame-Hart 500 under ambient conditions.

3. Results and discussion

3.1. Breath-figures patterning on the silicone oil lubricated solid substrates

Peer-reviewed version available at *Materials* **2019**, *12*, 3051; doi:10.3390/ma12183051

The drop-casting involves a diversity of physico-chemical events, namely 1) spreading of droplet; 2) evaporation of the polymer solution; 2) nucleation and condensation of water droplets; 4) growth and self-assembly of droplets; 5) evaporation of water; 6) solidification of polymer accompanied giving rise the eventual micro-porous pattern, as shown in **Figure 1** and discussed in detail in ref. 25. The capillary cluster, giving rise to the formation of the eventual breath-figures pattern is formed in the vicinity of the triple (three-phase) line, as shown in **Figure 2A**.

It was reported that the substrate has a crucial impact on the breath-figures self-assembly [17, 32-33]. In particular, it was suggested that thick solid substrates (with the thickness of *ca* 1mm), working at a thermal bath, stabilize the process of evaporation of polymer solution [34]. In our research we modified the wetting regime of the substrate by lubrication with the silicone oil. The wetting of lubricated solid surfaces is rich in its physical content [35-40]. Silicone oils are usually (but not necessarily) used for lubrication. When a liquid wets a surface lubricated with another liquid, different wetting regimes are possible [35-39]. Consider a high surface energy droplet (say, water) placed on a low surface energy liquid (say, silicone oil) lubricated surface. The oil may spread over and "cloak" the water droplet [35-39]. This is important because cloaking can stop an evaporation necessary for the breath figures-self-assembly. The criterion for coating ("cloaking") is given by Eq. 1:

$$\Psi = \gamma_{wa} - (\gamma_{ow} + \gamma_{oa}) > 0, \quad (1)$$

where Ψ is the spreading coefficient and γ_{wa}, γ_{wo} and γ_{oa} are the surface tensions at the water/air, oil/water and oil/air interfaces respectively [41, 42]. In the situation where $\Psi < 0$, the "non-coating" wetting regime takes place enabling the breath-figures self-assembly, and this was the case in our experiments, due to the relatively low surface tension of the polymer solution.

When droplets of polymer solution are placed on the glass slide and silicone lubricated glass slide they behave in very different ways, as illustrated in **Figure 2**. When a droplet is placed on the dry slide glass, the triple line is pinned, as shown in **Figure 2A**. Contrastingly, when is it is dripped on the lubricated slide the triple line is de-pinned and the droplet spreads and form the so-called "puddle" with the thickness of 70±10 μm, as depicted in **Figure 2B**.

The change of the wetting regime resulted in the dramatic change of eventual patterns, obtained with "dry" and silicone oil-lubricated substrates. The patterns arising from the drop-casting on dry glass slides are shown in **Figure 3**. The large-scale pattern with a characteristic lateral scale of 50 μm is recognized from the SEM image, supplied in **Figure 3A**. The origin of this pattern remains highly disputable and it was related the crack patterns [43] and also to the diversity of instabilities occurring in the evaporated polymer solutions [44-49]. In parallel, the honeycomb-microporous patterns, typical for the breath-figures self-assembly, were observed, as shown in **Figure 3B**. The pores, constituting the pattern, were disordered and demonstrated the high dispersion of their sizes.

The situation changed dramatically when the polymer solution was deposited on the silicone oil-lubricated substrates, as shown in **Figures 4A-C**. The aforementioned large-scale pattern disappeared. The honeycomb micro-porous pattern ordered pattern, depicted in **Figures 4A-C,** was observed. It should be emphasized that the pattern was hierarchical, namely small-scale nano-pores were located within "large" micro-scaled pores, as shown in **Figures 4 B-C**. The diameters of the nano-pores were established with SEM as 100-300 nm. The presence of nano-scaled pores makes the reported films suitable for ultra-filtration. Formation of the hierarchical porous structures under the breath-figures self-assembly was addressed in ref. 12. However, the precise mechanism of their formation remains obscure and calls for the future investigations. Hierarchical porous structures were registered with both PS ($M_w = 35.000$) and the industrial grade PS, as shown in **Figure 5**.

3.2. Characterization of ordering of the breath-figures pattern

Ordering of the pores was quantified with the Voronoi tessellations method. A Voronoi tessellation or diagram of an infinite plane is a partitioning of the plane into regions based on the distance to a specified discrete set of points called also *nuclei* (or generators [50-51]). For each seed, there is a corresponding region consisting of all points closer to that seed than to any other. The centers of the large micro-scaled pores depicted in **Figures 4A-B** were taken as *nuclei* (thus, the small-scale pores were ignored). The Voronoi entropy was calculated as:

$$S_{vor} = -\sum_n P_n \ln P_n \ , \qquad (2)$$

where P_n is the fraction of polygons with n sides or edges (also called the coordination number of the polygon) in a given Voronoi diagram [50-51]. The Voronoi entropy was successfully used for characterization of ordering in breath-figures patterns in refs. 52-55. The values of the Voronoi entropy $S_{vor} = 0.41 - 0.48$ were reported in ref. 10 for the breath-figures patterning, which are much lower than $S_{vor} = 1.71$, inherent for the random distrubutions of pores [55]; thus, evidencing the pronounced ordering of micro-pores. We established $S_{vor} = 0.6 - 0.9$ for the reported patterns (see **Figure 6**), also evidencing the ordering of pores. However, the observed ordering was far from to be comprehensive (consider, that $S_{vor} = 0$ for "ideal" ordering).

3.3. Characterization of wetting of the samples arising from the breath-figures self-assembly

Measurement of the apparent contact angles remains the simplest, inexpensive and reliable method of characterization of porous surfaces [41, 42]. The equilibrium contact angle of flat PS was established as $\theta = 86 - 88^0$ [56, 57]. The apparent contact angle of the porous topographies arising from the breath-figures self-assembly on oil-lubricated surfaces was established as $\theta^* = 100 - 107 \pm 1^0$, as shown in **Figure 7**. Thus, we conclude that the Cassie-Baxter air trapping regime is inherent for the reported patterns [41, 42]. Consider, that under the Wenzel wetting regime inherently hydrophilic substrate become more hydrophilic. Of course, the Cassie and Wenzel wetting models do not exhaust all possible wetting regimes, and more complicated wetting regimes are widespread on real surfaces, and the so called "mixed" wetting mode is possible for the reported patterns [42].

4. Conclusions

We conclude that the silicone oil lubricated substrates promote de-pinning of the triple line of droplets of polymer solutions and their spreading; thus, these substrates are especially suitable for the drop-casting process, resulting in the breath-figures self-assembly [12-17]. The drop-casting of polystyrene dissolved in the chlorinated solvents on the silicone oil-lubricated glass slides, carried out in the humid atmosphere, gave rise to hierarchical topographies built of micro- and nano-pores. The hierarchical topography was observed with the industrial grade polystyrene and polystyrene with the molecular

weight $M_w = 35.000$. The presence of nano-pores makes the reported films suitable for ultra-filtration applications. The ordering of the micro-pores was quantified with the Voronoi tessellations and calculation of the corresponding Voronoi entropy. The Voronoi entropy was established as $S_{vor} = 0.6 - 0.9$, which is much smaller than $S_{vor} = 1.71$ inherent for random 2D patterns [50-55]. Obtuse apparent contact angles established for the reported honeycomb films evidence the Cassie-Baxter air trapping wetting regime.

Acknowledgements

The authors are thankful to Dr. Irina Legchenkova for her kind help in preparing this paper.

References

1. Chen, C.S.; Mrksich, M.; Huang, S.; Whitesides, G.M.; Ingber, D.E. Micropatterned Surfaces for Control of Cell Shape, Position, and Function. *Biotechnol. Prog.* **1998**, *14*, 356–363.
2. Varenberg, M.; Gorb, S.N. Hexagonal Surface Micropattern for Dry and Wet Friction. *Adv. Mater.* **2009**, *21*, 483–486.
3. Xia, Y.; Kim, E.; Zhao, X.; Rogers, J.; Prentiss, M.; Whitesides, G.M. Complex optical surfaces formed by replica molding against elastomeric masters. *Science (80-.).* **1996**, *273*, 347–349.
4. Stone, H.A.; Kim, S. Microfluidics: Basic issues, applications, and challenges. *AIChE J.* **2001**, *47*, 1250–1254.
5. Koch, K.; Bhushan, B.; Barthlott, W. Multifunctional surface structures of plants: an inspiration for biomimetics. *Prog. Mater. Sci.* **2009**, *54*, 137–178.
6. Barthlott, W.; Neinhuis, C. Purity of the sacred lotus, or escape from contamination in biological surfaces. *Planta* **1997**, *202*, 1–8.
7. Wen, L.; Weaver, J.; Lauder, G. Biomimetic shark skin: design, fabrication and hydrodynamic function. *J. Exp. Biol.* **2014**, *217*, 1656–1666.
8. Liu, Y.; Li, G. A new method for producing “Lotus Effect” on a biomimetic shark skin. *J. Colloid Interface Sci.* **2012**, *388*, 235–242.
9. Falconnet, D.; Csucs, G.; Grandin, H.; Textor, M. Surface engineering approaches to micropattern surfaces for cell-based assays. *Biomaterials* **2006**, *27*, 3044–3063.
10. Rodríguez-Hernández, J. Wrinkled interfaces: Taking advantage of surface instabilities to pattern polymer surfaces. *Prog. Polym. Sci.* **2015**, *42*.

11. Rodríguez-Hernańdez, J.; Drummond, C. *Polymer surfaces in motion: Unconventional patterning methods*; **2015**; ISBN 9783319174310.

12. Muñoz-Bonilla, A.; Fernández-García, M.; Rodríguez-Hernández, J. Towards hierarchically ordered functional porous polymeric surfaces prepared by the breath figures approach. *Prog. Polym. Sci.* **2014**, *39*.

13. Escalé, P.; Rubatat, L.; Billon, L.; Journal, M.S.-E.P.; 2012, U. Recent advances in honeycomb-structured porous polymer films prepared via breath figures. *Eur. Polym. J.* **2012**, *48*, 1001–1025.

14. Bormashenko, E. Breath-figure self-assembly, a versatile method of manufacturing membranes and porous structures: Physical, chemical and technological aspects. *Membranes (Basel).* **2017**, *7*, 1–20.

15. Zhang, A.; Bai, H.; Li, L. Breath Figure: A Nature-Inspired Preparation Method for Ordered Porous Films. *Chem. Rev.* **2015**, *115*, 9801–9868.

16. Stenzel, M. H.; Barner-Kowollik, C.; Davis, Th. P. Formation of honeycomb-structured, porous films via breath figures with different polymer architectures. *J. Polym. Sci. A* **2006**, **44**, 2363- 2375.

17. Wan, L-S., Zhu, L-W., Ou, Y., Xu, Z-K. Multiple interfaces in self-assembled breath figures. **2014**, *Chem. Commun*. 50, 4024-4039 .

18. Beysens, D. Dew nucleation and growth. *Comptes Rendus Phys.* **2006**, *7*, 1082–1100.

19. Aitken, J. Breath Figures. *Nature* **1911**, *86*, 516–517.

20. Rayleigh Lord, Breath Figures. *Nature* **1912**, *90*, 436–438.

21. Baker, T.J. Breath Figures. *London, Edinburgh, Dublin Philos. Mag. J. Sci.* **1922**, *44*, 752–765.

23. Widawski, G.; Rawiso, M.; François, B. Self-organized honeycomb morphology of star-polymer polystyrene films. *Nature* **1944**, *369*, 387–389.

24. François, B.; Pitois, O.; François, J. Polymer films with a self-organized honeycomb morphology. *Adv. Mater.* **1995**, *7*, 1041–1044.

25. Maruyama, N.; Koito, T.; Nishida, J.; Sawadaishi, T.; Cieren, X.; Ijiro, K.; Karthaus, O.; Shimomura, M. Mesoscopic patterns of molecular aggregates on solid substrates. *Thin Solid Films* **1998**, *327–329*, 854–856.

26. Bunz, U.H.F. Breath Figures as a Dynamic Templating Method for Polymers and Nanomaterials. *Adv. Mater.* **2006**, *18*, 973–989.

27. Srinivasarao, M.; Collings, D.; Philips, A.; Patel, S. Three-dimensionally ordered array of air bubbles in a polymer film. *Science* **2001**, *292*, 79-83.

28. Park, M. S.; Kim, J. K. Broad-band antireflection coating at near-infrared wavelengths by a breath figure. *Langmuir* **2005**, *21*(24) 11404-11408.
29. Yabu, H.; Shimomura, M. Simple fabrication of micro lens arrays. *Langmuir* **2005**, *21*(5), 1709-1711.
30 Mansouri, J.; Yapit, E.; Chen, V. Polysulfone filtration membranes with isoporous structures prepared by a combination of dip-coating and breath figure approach. *J. Membrane Sci*. **2013**, *444*, 237-251.
31. Castaño, M.; Martinez-Campos, E.; Pintado-Sierra, M.; García, C.; Reinecke, H.; Gallard, A.; Rodriguez-Hernandez, J.; Elvira C. Combining breath figures and supercritical fluids to obtain porous polymer scaffolds. *ACS Omega* **2018**, *3*(10) 12593-12599.
32. Ferrari, E.; Fabbri, P.; Pilati, Fr. Solvent and substrate contributions to the formation of breath figure patterns in polystyrene films. *Langmuir* **2011**, *27* (5), 1874–1881.
33. Bormashenko, E.; Pogreb R., Stanevsky O., Bormashenko Y., Stein T., Gaisin V.-Z., Cohen R., Gendelman O. Mesoscopic patterning in thin polymer films formed under the fast dip-coating process. *Macromol. Mater. Eng.* **2005**, 290, 114-121.
34. Ed. Bormashenko, Correct values of Rayleigh and Marangoni numbers for liquid layers deposited on thin substrates, *Ind. Eng. Chem. Res.* **2008**, 47 (5) 1726–172.
35. Daniel, D., Timonen, J. V. I., Li, R., Velling, S. J. & Aizenberg, J. Oleoplaning droplets on lubricated surfaces. *Nature Physics* **2017**, 13, 1020-1026.
36. Smith, J. D., Dhiman, R., Anand, S., Reza-Garduno, E., Cohen, R. T., McKinley, G, H. & Varanasi, K. R. Droplet mobility on lubricant-impregnated surfaces. *Soft Matter* **2013**, 6, 1772-1780.
37. Schellenberger, F., Xie, J., Encinas, N., Hardy, A., Klapper, M., Papadopoulos, P., Butt, H-J. & Vollmer, D. Direct observation of drops on slippery lubricant-infused surfaces. *Soft Matter* **2015**, 11, 7617-7626.
38. Nosonovsky M. Slippery when wetted, *Nature* **2011**, volume 477, pages 412–413 ()
39. Bormashenko Ed. Physics of pre-wetted, lubricated and impregnated surfaces: a review, *Phil.Trans.R.Soc.* **2019**, A, 377, 20180264.

40. Miranda, D. F., Urata, Ch., Masheder, B., Dunderdale, G. J., Yagihashi, M. & Hozumi, A. Physically and chemically stable ionic liquid-infused textured surfaces showing excellent dynamic omniphobicity. *APL Materials 2* **2014**, 056108.
41. de Gennes P. G., Brochard-Wyart F.& Quéré, D. *Capillarity and Wetting Phenomena*; Springer, Berlin, **2003**.
42. Bormashenko, Ed. *Physics of wetting: phenomena and applications of liquids on surfaces*, Ch. 2, 7, 10, De Gruyter, Berlin, **2017**.
43. Weh, L., Ventur, A. Crack patterns in thin polymer layers. *Macromol. Mater. Eng.* **2004**, 289, 227-237.
44. Fowler, P. D., Ruscher, C., McGraw, J. D. James, Forrest, J. A, Dalnoki-Veress, K. Controlling Marangoni-induced instabilities in spin-cast polymer films: How to prepare uniform films. *Eur. Phys. J.* **2016**, E 39, 90.
45. Nilavarasia, K., Madhurima, V. Controlling breath figure patterns on PDMS by concentration variation of ethanol-methanol binary vapors. *Eur. Phys. J.* **2018**, E 41, 82.
46. Bormashenko E., Pogreb R., Stanevsky O., Bormashenko Y., Stein T., Gendelman O. Mesoscopic patterning in evaporated polymer solutions: New experimental data and physical mechanisms, *Langmuir* **2005**, 21, 9604-9609.
47. Bormashenko, Ed., Pogreb, R. Musin, A., Stanevsky, O., Bormashenko, Ye. Whyman, G., Gendelman, O., Barkay, Z. Self-assembly in evaporated polymer solutions: Influence of the solution concentration. *Journal of Colloid and Interface Science* **2006**, 297 () 534–540.
48. P.G. De Gennes, Instabilities during the evaporation of a film: Non-glassy polymer + volatile solvent *Eur. Phys. J.* **2001**, E 6, 421–424.
49. P.G. De Gennes, Solvent evaporation of spin cast films: "crust" effects. *Eur. Phys. J* **2002**, E 7 31–34.
50. Barthélemy, M. Spatial networks. *Phys. Rep.* **2011**, 499 (1-3), 1–101, doi:10.1016/j.physrep.2010.11.002.
51. Bormashenko, Ed., Frenkel M., Vilk A., Legchenkova I., Fedorets, A.A., Aktaev, N. E., Dombrovsky L. A., Nosonovsky M. Characterization of Self-Assembled 2D Patterns with Voronoi Entropy. *Entropy* **2018**, 20(12), 956.

52. Park, M. S.; Kim, J. K. Breath figure patterns prepared by spin coating in a dry environment. *Langmuir* **2004** 20 (13), 5347-5352.

53. Escalé P., Save M., Billon L,, Ruokolainen J., Rubatat L. When block copolymer self-assembly in hierarchically ordered honeycomb films depicts the breath figure process., *Soft Matter* **2016**, 12, 790-797.

54. Madej, W.; Budkowski, A.; Raczkowska, J.; Rysz, J. Breath figures in polymer and polymer blend films spin-coated in dry and humid ambience. *Langmuir* **2008**, 24 (7), 3517-3524.

55. Limaye, A. V.; Narhe, R. D.; Dhote, A. M.; Ogale, S. B. Evidence for convective effects in breath figure formation on volatile fluid surfaces. *Phys. Rev. Lett.* **1996**, 76 (20), 3762-3765.

56. Yuan Li, J. Q. Pham, K. P. Johnston, P. F. Green, Contact Angle of Water on Polystyrene Thin Films: Effects of CO2 Environment and Film Thickness, *Langmuir* **2007**, 23(19), 9785-9793

57. Kwok, D. Y.; Lam, C. N. C.; Li, A.; Zhu, K.; Wu, R.; Neumann, A. W. Low-rate dynamic contact angles on polystyrene and the determination of solid surface tensions, *Polym. Eng. Sci*.**1998**, 38, 1675

Peer-reviewed version available at *Materials* **2019**, *12*, 3051; doi:10.3390/ma12183051

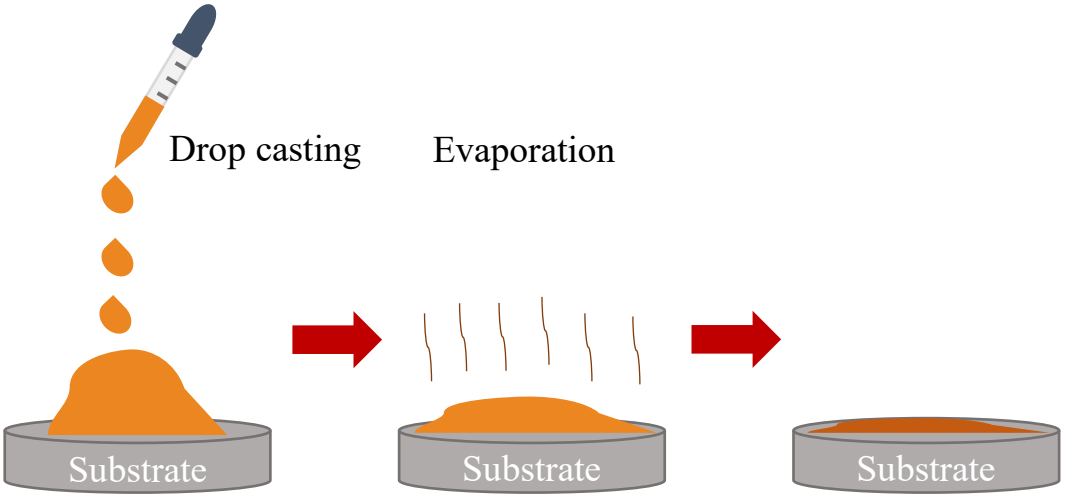

Figure 1. Sketch of the drop-casting process is depicted.

Peer-reviewed version available at *Materials* **2019**, *12*, 3051; doi:10.3390/ma12183051

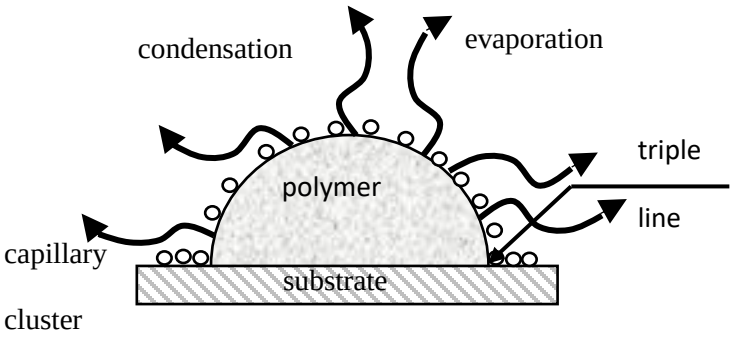

Figure 2A. Breath-figures self-assembly taking place under drop casting is depicted. A droplet of the polymer solution is evaporated in the humid atmosphere. Water droplets are condensed at the polymer solution/vapor interface. A capillary cluster built from water droplets is formed in the vicinity of the triple (three-phase) line.

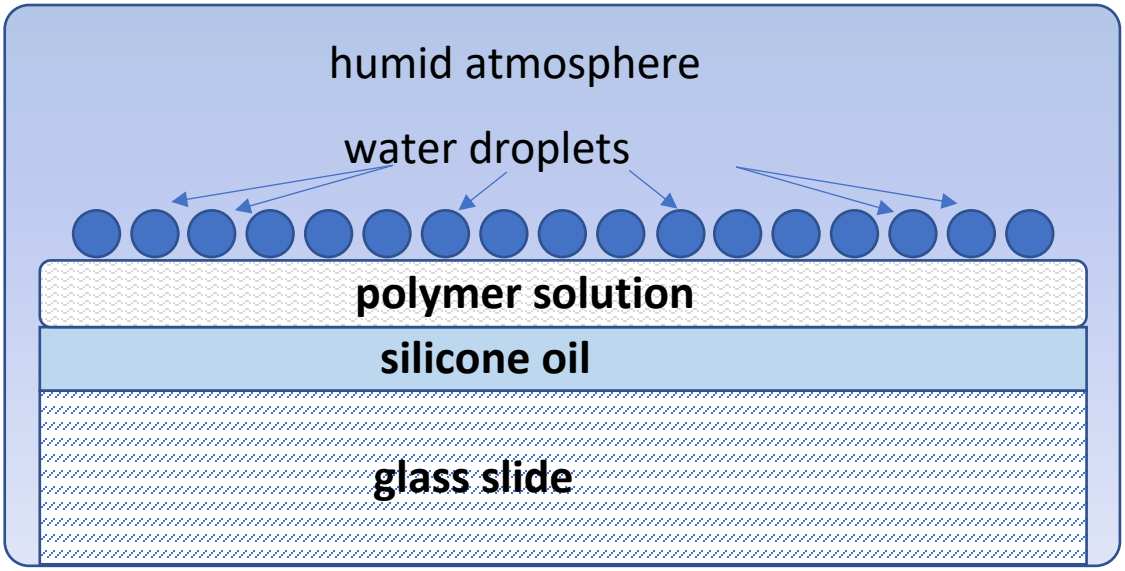

Figure 2B. Breath-figures self-assembly taking place under drop casting on silicone oil lubricated surfaces is shown. Silicone oil promotes spreading of the polymer solution evaporated in the humid atmosphere.

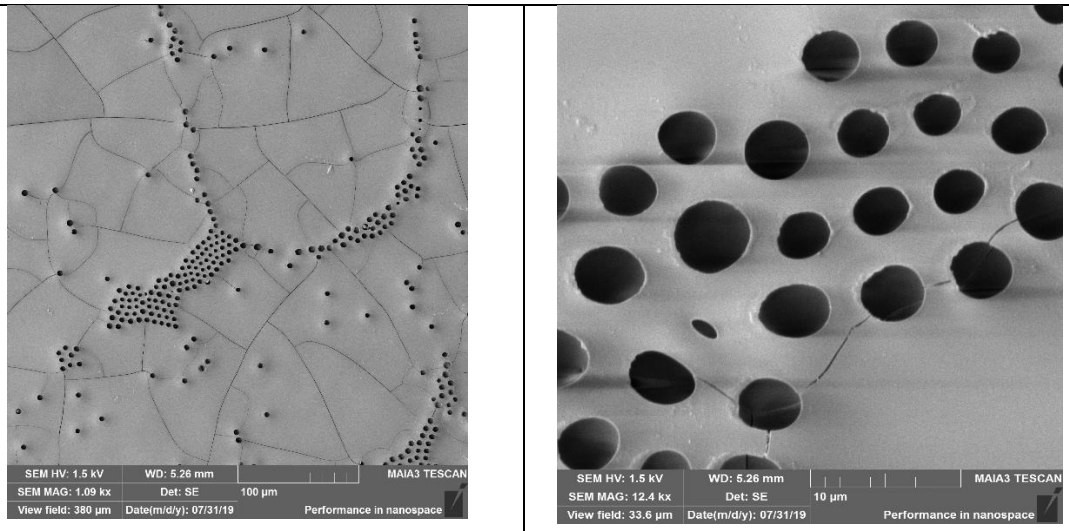

A B

Figure 3. SEM images of breath figures patterns obtained with drop-casting on the non-lubricated substrates are presented. A. Scale bar is 100 µm. B. Scale bar is 10 µm.

Preprints (www.preprints.org) | NOT PEER-REVIEWED | Posted: 13 August 2019 doi:10.20944/preprints201908.0153.v1

Peer-reviewed version available at *Materials* **2019**, *12*, 3051; doi:10.3390/ma12183051

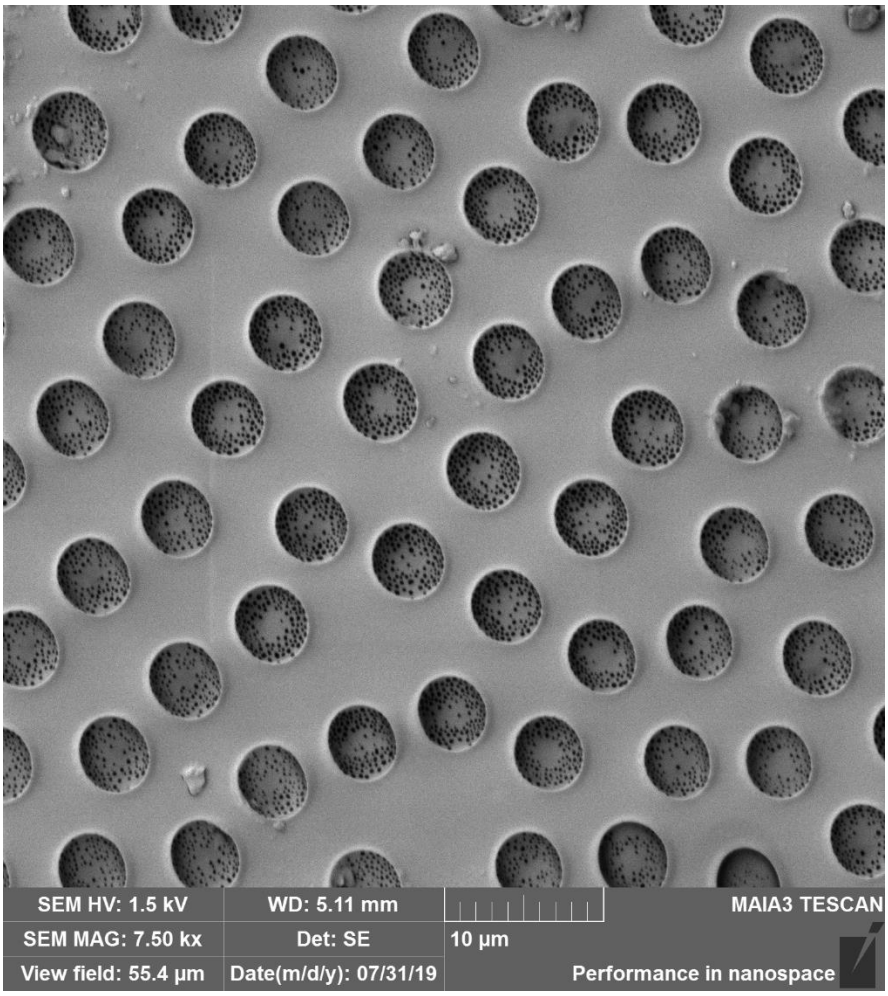

Figure 4A. SEM image of the breath figures pattern obtained with silicone oil lubricated substrates. The solution of PS with molecular mass $M_w = 35.000$ was used for the breath-figures self-assembly. The scale bar is is 10 µm.

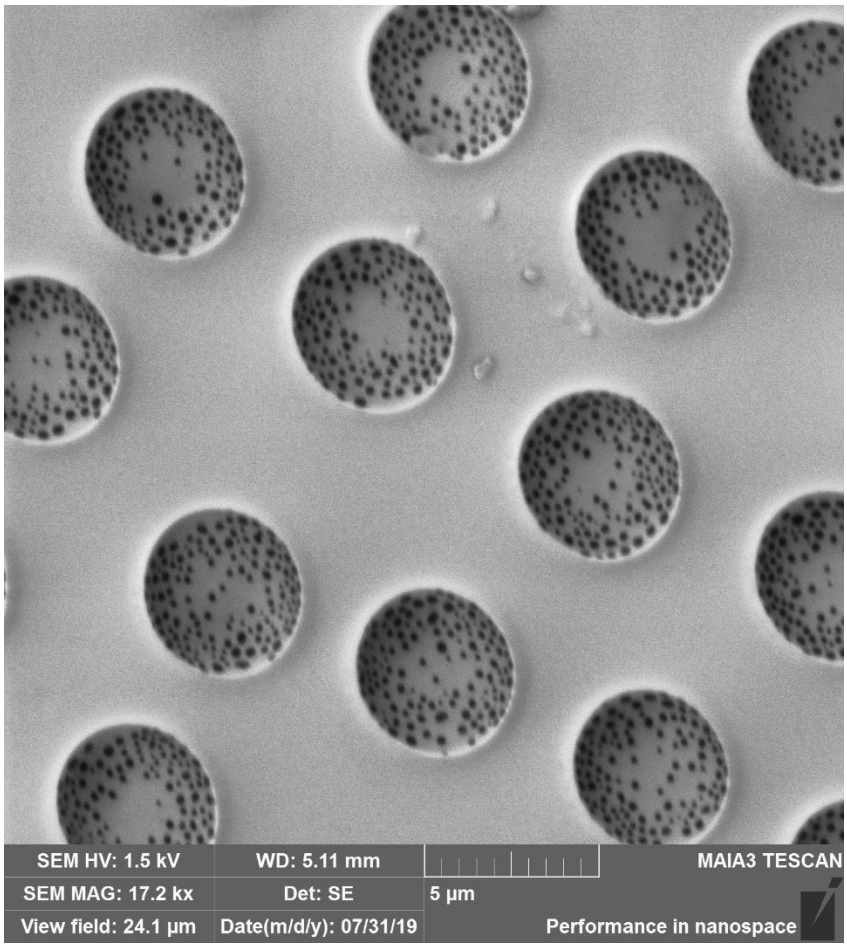

Figure 4B. The large-scale SEM image of the breath figures pattern obtained with silicone oil lubricated substrates is shown. The scale bar is 5µm.

Preprints (www.preprints.org) | NOT PEER-REVIEWED | Posted: 13 August 2019 doi:10.20944/preprints201908.0153.v1

Peer-reviewed version available at *Materials* **2019**, *12*, 3051; doi:10.3390/ma12183051

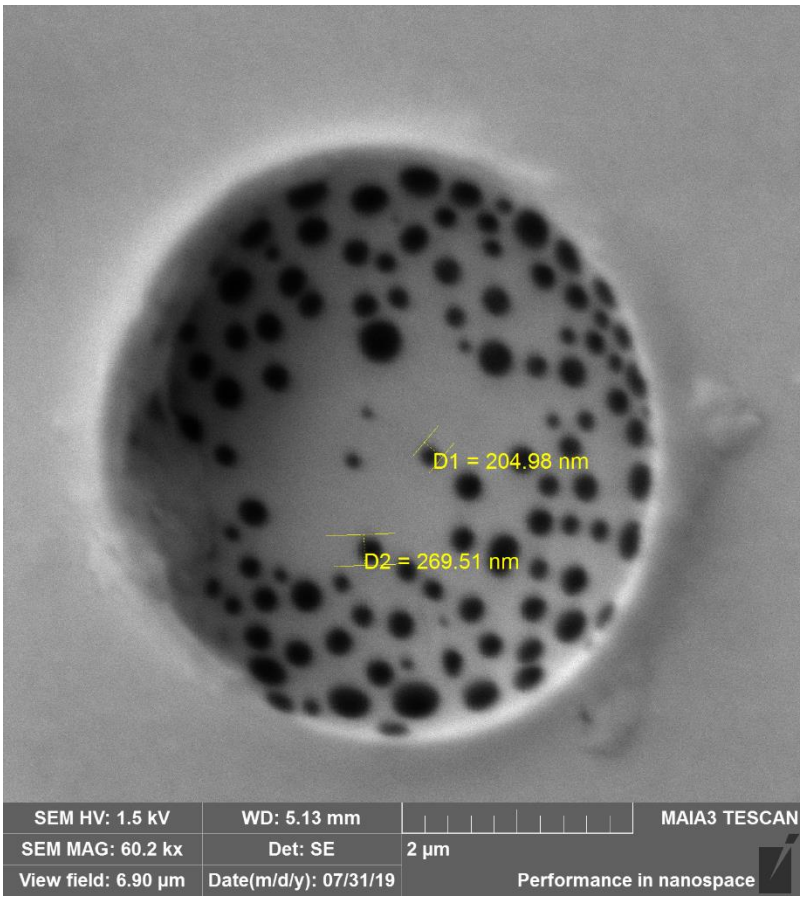

Figure 4C. The large-scale SEM image of the pore is depicted. The scale bar is 2 µm. Nano-pores are clearly seen.

Preprints (www.preprints.org) | NOT PEER-REVIEWED | Posted: 13 August 2019 doi:10.20944/preprints201908.0153.v1

Peer-reviewed version available at *Materials* **2019**, *12*, 3051; doi:10.3390/ma12183051

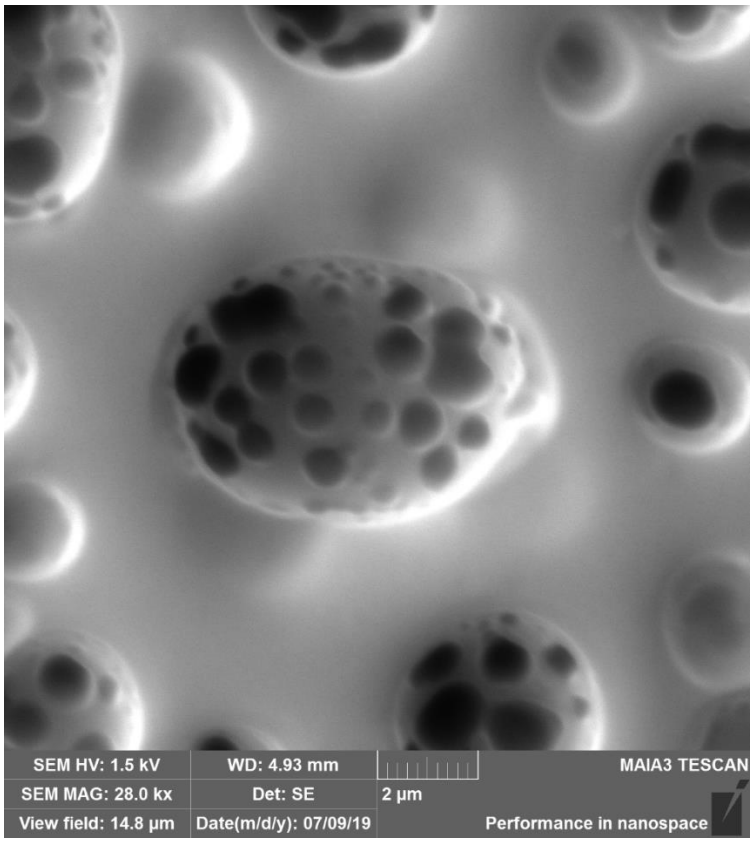

Figure 5. SEM image of the breath figures pattern obtained with silicone oil lubricated substrates is depicted. The solution of industrial PS was used for the breath-figures self-assembly. The scale bar is 2µm.

Preprints (www.preprints.org) | NOT PEER-REVIEWED | Posted: 13 August 2019 doi:10.20944/preprints201908.0153.v1

Peer-reviewed version available at *Materials* **2019**, *12*, 3051; doi:10.3390/ma12183051

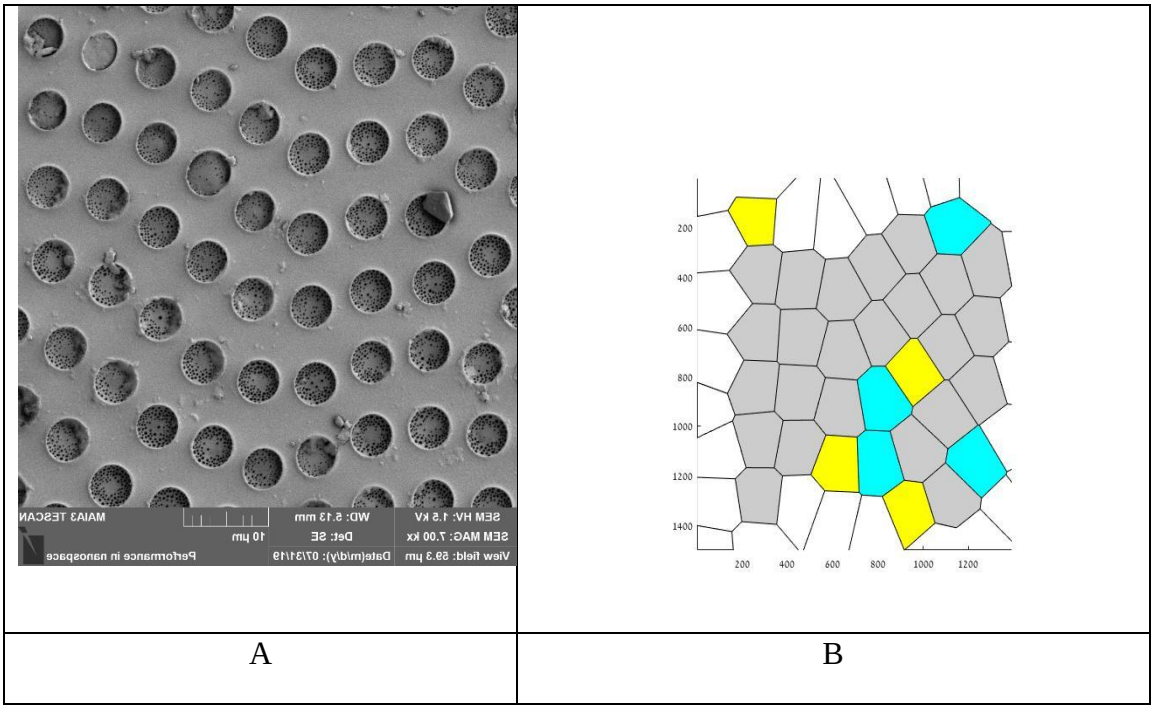

A B

Figure 6. The SEM image of the honeycomb pattern (A) and the appropriate Voronoi tessellation (B) are shown. The calculated Voronoi entropy S_{vor} =0.736.

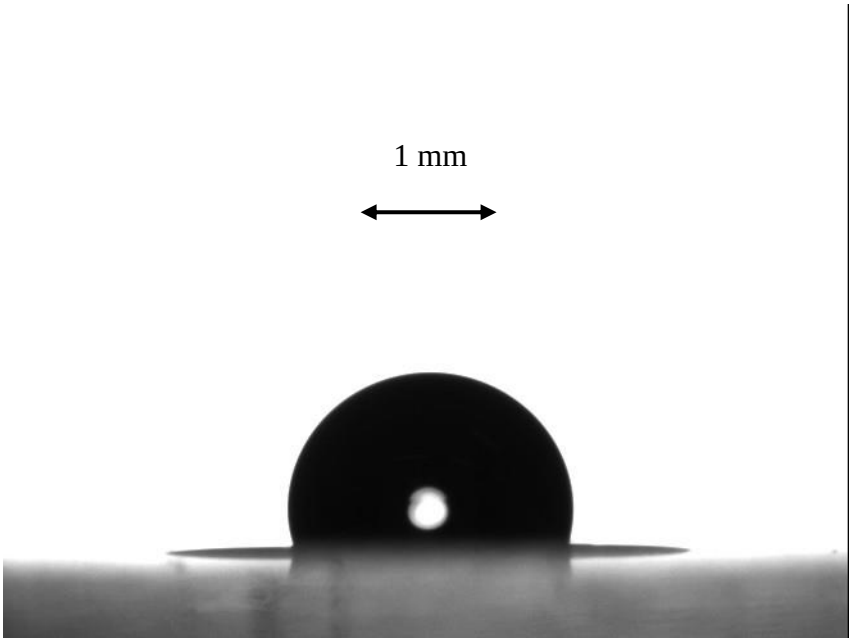

Figure 7. Obtuse apparent water contact angle measured on PS honeycomb surfaces, obtained under breath-figures self-assembly with oil-lubricated solid surfaces is shown. The volume of water droplet is 5 µl. The scale bar is 1 mm.